Subsystem macroarchitecture of the intrinsic midbrain neural network and its tectal and tegmental subnetworks

Larry W. Swanson[a,1], Joel D. Hahn[a], and Olaf Sporns[b,c]

[a]Department of Biological Sciences, University of Southern California, Los Angeles, CA 90089; [b]Indiana University Network Science Institute, Indiana University, Bloomington, IN 47405; and [c]Department of Psychological and Brain Sciences, Indiana University, Bloomington, IN 47405

Contributed by Larry W. Swanson, April 9, 2021 (sent for review February 5, 2021; reviewed by Paul E. Micevych and Robert Vertes)

The midbrain is the smallest of three primary vertebrate brain divisions. Here we use network science tools to reveal the global organizing principles of intramidbrain axonal circuitry before adding extrinsic connections with the remaining nervous system. Curating the experimental neuroanatomical literature yielded 17,248 connection reports for 8,742 possible connections between the 94 gray matter regions forming the right and left midbrain. Evidence for the existence of 1,676 connections suggests a 19.2% connection density for this network, similar to that for the intraforebrain network [L. W. Swanson *et al.*, Proc. Natl. Acad. Sci. U.S.A. 117, 31470–31481 (2020)]. Multiresolution consensus cluster analysis parceled this network into a hierarchy with 6 top-level and 30 bottom-level subsystems. A structure–function model of the hierarchy identifies midbrain subsystems that play specific functional roles in sensory–motor mechanisms, motivation and reward, regulating complex reproductive and agonistic behaviors, and behavioral state control. The intramidbrain network also contains four bilateral region pairs designated putative hubs. One pair contains the superior colliculi of the tectum, well known for participation in visual sensory–motor mechanisms, and the other three pairs form spatially compact right and left units (the ventral tegmental area, retrorubral area, and midbrain reticular nucleus) in the tegmentum that are implicated in motivation and reward mechanisms. Based on the core hypothesis that subsystems form functionally cohesive units, the results provide a theoretical framework for hypothesis-driven experimental analysis of neural circuit mechanisms underlying behavioral responses mediated in part by the midbrain.

behavioral state | connectomics | motivation | neuroinformatics | reward

According to the classical view, early in vertebrate development the neural plate invaginates to form the neural tube, which immediately displays three sequential swellings that were called the primary forebrain, midbrain (MB), and hindbrain vesicles by von Baer in 1837 (1) and that are followed by the presumptive spinal cord caudally. Together, these four differentiations or morphogenetic units of the neural tube go on to generate the entire adult central nervous system (2, 3). As a major part of a systematic research program to analyze the organizing principles of mammalian nervous system macroconnectivity, we recently completed a study of forebrain intrinsic circuitry (4), and here we present a similar study of MB intrinsic circuitry.

Based on developmental and adult topographic features, the MB can be divided into two great parts: tectum (TC) dorsally and tegmentum (TG) ventrally (5, 6). In mammals, the TC in turn has two parts, the superior and inferior colliculi, which are important nodes in circuitry related to visual and auditory functions, respectively (3). The TG, in contrast, is much more differentiated structurally and functionally, with a variety of gray matter regions that have been intensively analyzed over the last 75 y. Among the most prominent are three cranial nerve nuclei (oculomotor nucleus, trochlear nucleus, and midbrain nucleus of the trigeminal nerve), as well as the pretectal region, red nucleus, substantia nigra and ventral tegmental area, midbrain raphe nuclei, periaqueductal gray, and midbrain reticular nucleus (3).

This topographic approach to biological structure–function organization is like dividing the body in human anatomy into head, neck, trunk, and upper and lower limbs with hands and feet. Topographic anatomy is particularly useful for describing and mapping structure–function spatial relationships of body parts and for surgical procedures. For example, the hand is an obvious body part with especially important and intricate functions in humans. Systems anatomy, however, is an equally valid and complementary way of describing global principles of body organization. In human biology, the body is conveniently and systematically divided into about a dozen interrelated systems (skeletal, digestive, respiratory, nervous, and so on), and components of each typically play a role in topographic parts such as the hand. The systems approach is particularly useful for organizing vast amounts of data into simplified, readily understandable conceptual frameworks or models of how the body works as a whole.

The nervous system can also be treated from the complementary topographic and systems perspectives (7), and it is the only bodily system remaining without a relatively simple global systems model, largely because its cellular network architecture is much more complex than the other systems. However, general network analysis tools, which can be applied to any complex system, from the internet to social interactions in a human population, offer one promising approach (8, 9). Basic requirements include a systematic parts list for the network, an understanding of how each part works,

Significance

The midbrain is one of the vertebrate brain's three basic divisions, and it plays an especially important role in sensory–motor mechanisms, motivation and reward, reproductive and agonistic behaviors, and behavioral state. Network science methods were applied here to reveal organizing principles of intramidbrain circuitry, which include a hierarchy of subsystems that was used to construct a structure–function model of the circuitry. The results show fundamental differences between intramidbrain and previously determined intraforebrain network organization and provide a theoretical framework for experimental analysis of intramidbrain circuit involvement in specific behaviors.

Author contributions: L.W.S. designed research; L.W.S. performed research; L.W.S., J.D.H., and O.S. analyzed data; L.W.S. wrote the paper; and J.D.H. and O.S. helped revise the manuscript.

Reviewers: P.E.M., David Geffen School of Medicine at UCLA; and R.V., Florida Atlantic University.

The authors declare no competing interest.

[1]To whom correspondence may be addressed. Email: larryswanson10@gmail.com.

This article contains supporting information online at https://www.pnas.org/lookup/suppl/doi:10.1073/pnas.2101869118/-/DCSupplemental.

Published May 12, 2021.

and an account of how the parts are connected to form a functional system (10). Our long-term strategy for the rat nervous system follows the time-honored approach to solving any difficult problem, that is, to proceed from coarser-grained to finer-grained analyses, analogous to the strategy used to sequence the human genome (11). Thus, using a nested approach, we have started at the coarse-grained macro level of analysis (axonal macroconnections from one gray matter region to another gray matter region), as a prelude and framework for analyses at the finer-grained meso level (connections between neuron types making up each gray matter region), micro level (connections between individual neurons making up each neuron type), and nano level (the set of synapses formed by each neuron) (12).

Results

Analysis Framework. Our overall strategy is based on the embryological (Fig. 1*A*) and topographic first principles mentioned in the Introduction. We began systematically to collate and analyze each of the 10 main subdivisions of the adult central nervous system (Fig. 1*B*) (5, 6) by starting rostrally with the cerebral cortex (13, 14) and cerebral nuclei (15). For this paper we have analyzed the intrinsic circuitry of the TC, TG, and TC and TG combined—the MB (Fig. 1 *C* and *D*). The analysis itself is based on experimental pathway-tracing data for connection presence (with direction and weight) or absence between all 47 gray matter regions (nodes) on the right and left sides of the MB in our rat brain reference atlas (16) (Dataset S1 for abbreviations and *SI Appendix, Materials and Methods* for one modification), described with defined vocabularies for axonal connections (7, 17) and mammalian gray matter regionalization (6). Connection reports were expertly collated from the primary structural neuroscience literature by L.W.S. as described in detail elsewhere (ref. 4; also see *SI Appendix, Materials and Methods*). A comparison of collations by two experts for the same connection matrix (intracerebral cortical network) is provided in ref. 14.

The number of possible intra-MB connections on one side of the brain (ipsilateral, uncrossed, or association connections) is 2,162 ($47^2 - 47$; intraregional connections are ignored), and the number of possible MB connections to the other side (contralateral, crossed, or commissural) is 2,209 (47^2), making 8,742 possible intra-MB connections bilaterally. Unlike the case for the forebrain (4), our systematic MB collation identified no statistically significant female–male connectional differences. In addition, no statistically significant right/left (or strain) MB connectional differences were found. Thus, all ipsilateral and contralateral connections were assigned to one side, and the same dataset was used for the other side. As a result, our analysis applies generally to the species level (adult rat, *Rattus norvegicus domestica*).

A dataset of 8,624 connection reports (19 columns of metadata/report) for ipsilateral and contralateral connections from the MB on one side was collated from 142 original research publications appearing since 1977, for 4,371 possible connections (with no right/left differences, doubled values are 17,248 connection reports for 8,742 possible connections for both sides). The connection reports were from 34 journals, book articles, or theses (46.4% from the *Journal of Comparative Neurology*) involving about 106 laboratories. Overall, 18 different pathway-tracing methods were used in generating connection reports; these and other metadata for each report are in Dataset S2.

Basic Connection Numbers and Data Validity. Because the TC and TG together form the MB, we will begin here with an overview of the entire intra-MB connection matrix. The next section begins with a cluster analysis of the simplest subconnectome, that for

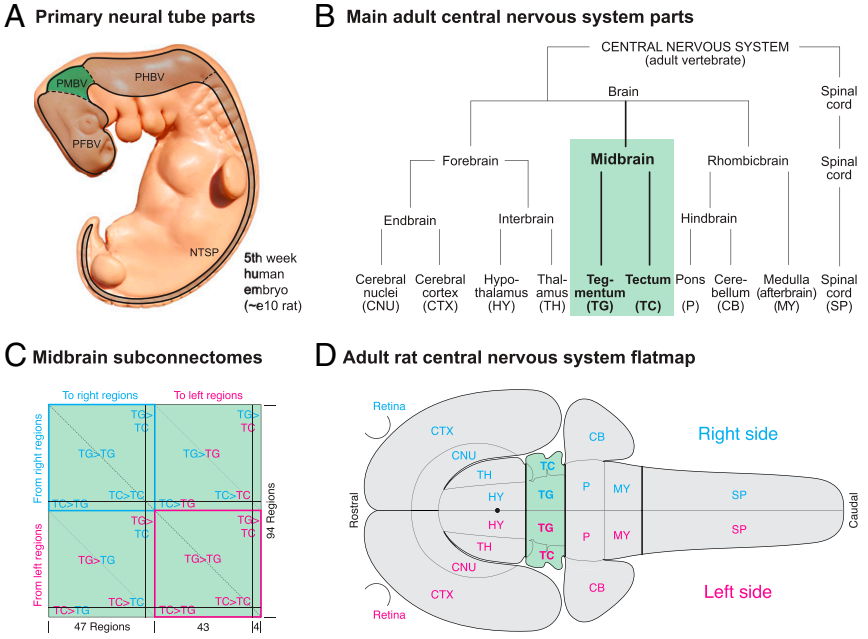

Fig. 1. Analysis strategy overview. (*A*) Schematic outline of the early neural tube, with its primary forebrain vesicle (PFBV), primary midbrain vesicle (PMBV), primary hindbrain vesicle (PHBV), and spinal cord part of neural tube (NTSP), superimposed on a model of the human embryo (as an exemplar for vertebrates). A qualitatively similar arrangement is a feature of all vertebrates at an equivalent stage of development. (*B*) Hierarchy of major central nervous system subdivisions common to adult vertebrates. Note that the PHBV (*A*) becomes the adult rhombicbrain, and that the adult hindbrain has a more restricted meaning than in the early neural tube; see ref. 6. (*C*) Schematic view of the adult rat bilateral MB connection matrix (MB2) with the 16 subconnectomes formed by the tegmentum (TG) and tectum (TC) on each side. The MB2 matrix has 94 rows and 94 columns (47 for the MB on each, with 43 for TG and 4 for TC, as indicated). The bilateral TG matrix alone is an 86×86 matrix, the bilateral TC matrix alone, an 8×8 matrix. The dashed line from *Upper Left* to *Lower Right* is the main diagonal, indicating the connection of a region to itself, with no value in a macroconnectome where regions are treated as black boxes. The two shorter diagonals (lighter dashed lines) parallel to the main diagonal represent homotopic crossed connections: from a region on one side of the brain to the corresponding region on the other side. (*D*) The right and left midbrain (MB), consisting of TG and TC, shown on a rat central nervous system flatmap (22).

the TC, with just an 8 × 8 connection matrix. This is followed by an analysis of the TG subconnectome (86 × 86 connection matrix), and then the full MB subconnectome (94 × 94 connection matrix).

For the intra-MB connection matrix as a whole, the collation identified 486 ipsilateral connections as present and 1,463 as absent, a 24.9% connection density. As before (4), "unclear" values are binned with "absent" values, "axons-of-passage" are binned conservatively with "weak," and "present" are binned with "moderate." In contrast, 352 contralateral intra-MB connections from one side were identified as present and 1,586 as absent (18.2% connection density). Thus, for each MB side, 838 ipsilateral and contralateral connections were identified as present, and 3,049 as absent (21.6% connection density); these numbers are doubled for the complete bilateral intra-MB connection matrix (connection density also 21.6%, because no right/left differences; a surprising 99.98% of the connection reports used for analysis did not report which MB side was microinjected with pathway tracer).

No published data were found for 213 (9.8%) of all 2,162 possible ipsilateral intra-MB connections for a matrix coverage (fill ratio) of 90.2% (Fig. 2, *Left* column), whereas matrix coverage for contralateral connections was 87.7% (no article found for 271 of 2,209 possible connections). Thus, matrix coverage for all ipsilateral and contralateral connections arising in one MB is 88.9%, which also applies to the complete bilateral intra-MB connection matrix (with no right/left differences).

Assuming the connection reports representatively sample the 47-region matrix for each MB side, a complete ipsilateral intra-MB connection matrix would contain ∼539 connections, a complete contralateral intra-MB connection matrix would contain ∼401 connections, and the complete bilateral intra-MB connection matrix would contain ∼1,885 connections.

For network analysis, reported connection-weight values of "no data" and unclear were binned with absent values (see Dataset S6, layer F), and all values were converted from the descriptive ordinal scale to a $\log_{10}$ scale covering five orders of magnitude (see Dataset S6, layer G), the reported range of rat connectional data (4) (Fig. 2, *Middle* column). The resulting connection densities for ipsilateral and contralateral intra-MB connections are: ipsilateral, 22.5%; contralateral, 15.9%; and both ipsilateral and contralateral, 19.2% (Dataset S3). For the complete set of bilateral MB regions, the range of ipsilateral and contralateral output connections (the output connection degree range) is 0 to 63, the input connection degree range is 0 to 62, and the total (input + output) degree range is 2 to 122.

A validity metric was applied to the pathway-tracing method associated with each connection report (4). The metric uses an ordinal seven-point scale (1 to 7/lowest to highest validity). Using this approach, the following average validity values were determined for the data that were used for network analysis: for connections reported to exist, ipsilateral (within one side) = 6.18, contralateral (between sides) = 6.10, and within and between sides = 6.15; for connections reported to not exist, ipsilateral = 6.05, contralateral = 5.98, and both = 6.01 (Fig. 3 and Datasets S2 and S6, layers D and I).

Subsystem Analysis. Our first approach to clarify organizing principles of nervous system circuitry has been to examine its subsystem (SS) architecture with multiresolution consensus cluster (MRCC) analysis (18, 19). It is designed to detect strongly connected clusters (called communities, modules, or the synonym used here, subsystems) among the directed and weighted axonal connections between all regions (nodes) of the network represented in a connection matrix (connectome)—across all levels of partitioning resolution or scale (1 to 94 possible levels for MB2). The result identifies without preconceived biases (agnostically) variously sized clusters that are arranged hierarchically, thus generating a compact description of all nested SSs and their interactions (Fig. 2, *Right* two columns). For this paper, MRCC analysis was applied to the complete bilateral (94 × 94 region) intra-MB connection matrix (MB2) and to the bilateral submatrices, intraTG (TG2) and intraTC (TC2) (Fig. 1*C*).

It is instructive to begin with the TC because, with only eight regions (four on each side of the brain), it has by far the smallest connection matrix of the 10 major central nervous system subdivisions (Fig. 1*B*)—the next smallest is the cerebellum with 40—and because MRCC analysis yields a very simple solution (Fig. 2, *Top* row, *Right* two columns). The TC2 cluster tree has just three branches or subsystems associated with one level: one subsystem is bilateral and consists of two regions, the right and left superior colliculi (SC), whereas the other two subsystems are mirror images, each consisting of three regions (the three parts of the inferior colliculus [IC], on the right and left sides). As observed from the TC2 connection matrices (see Fig. 2, *Top* row, *Left* two columns; and Dataset S4, for interactive exploration of TC2 matrices), the right and left SC are more strongly connected with each other, through the commissure of superior colliculus, than with any of the IC regions, whereas the three IC parts on one side are more strongly interconnected with each other than with the three IC parts on the other side, or with either SC.

It is also important to note from the connection matrices that although subsystems consist of sets of the most strongly interconnected regions in a network of interest, each of the three TC2 subsystems are also interconnected (Fig. 2, *Top* row, *Left* two columns; and Dataset S4). Thus, MRCC analysis yields a set of interacting subsystems. These results for TC2 are not surprising; it has long been known that the tectum consists of pairs of superior and inferior colliculi that form quite distinct but interconnected structure–function units (3, 5).

The ventral MB subdivision, the TG, is much more differentiated than the TC: it has 43 bilaterally symmetrical regions on each side of the brain as compared to just 4 bilaterally symmetrical regions on each side. MRCC analysis also yields a more complex subsystem hierarchy for TG2 (Fig. 2, *Middle* row, *Right* two columns)—it has 7 top-level subsystems and 18 bottom-level subsystems that are arranged in 11 levels. The regional composition of these subsystems, and a more detailed, interactive view of the subsystem hierarchy form, including its levels, are presented in Dataset S5; the possible functional significance of the subsystem hierarchy is considered in *Hierarchical Structure–Function Subsystem Models* below.

It is well known that changing a brain network's anatomical coverage by adding (or subtracting) subconnectomes commonly alters network features of the component subconnectomes (4, 15, 19). This phenomenon is obvious when the TC2 and TG2 subconnectomes (Fig. 1*C*) are combined to form the 94 × 94 region MB2 subconnectome (Fig. 2, *Bottom* row). Here, MRCC analysis reveals a cluster tree with 6 top-level subsystems, 30 bottom-level subsystems, and 50 unique subsystems (hierarchy branches) in all, arranged in 21 levels (Dataset S6, layers B, D, and H).

This arrangement suggests the potential for a rich (50 × 50) set of interactions between all subsystem pairs that may be quantitated by comparing weighted connection densities (WCDs; the sum of all connection weights, including absent values, in a subsystem/number of regions in the subsystem) within and between all subsystem pairs (4). The resulting matrix (Dataset S6, layer J) displays 2,500 (50 × 50) possible subsystem interactions, compared with 8,742 possible connections in the MB2 system, thus providing a level of simplification to the network description. Furthermore, the individual subsystems are associated with a set of metrics derived from the original connection matrix, including size or number of constituent nodes (regions), persistence or stability in the hierarchy, WCD of intrinsic connections, ratio of intrinsic/extrinsic WCDs, ratio of input-to-output connections, and density of reciprocal connections (*SI Appendix*, Fig. S1).

Hierarchical Structure–Function Subsystem Models. Previous analyses suggest that the possible functional significance of some MRCC-generated subsystem cluster trees is more apparent than others, a

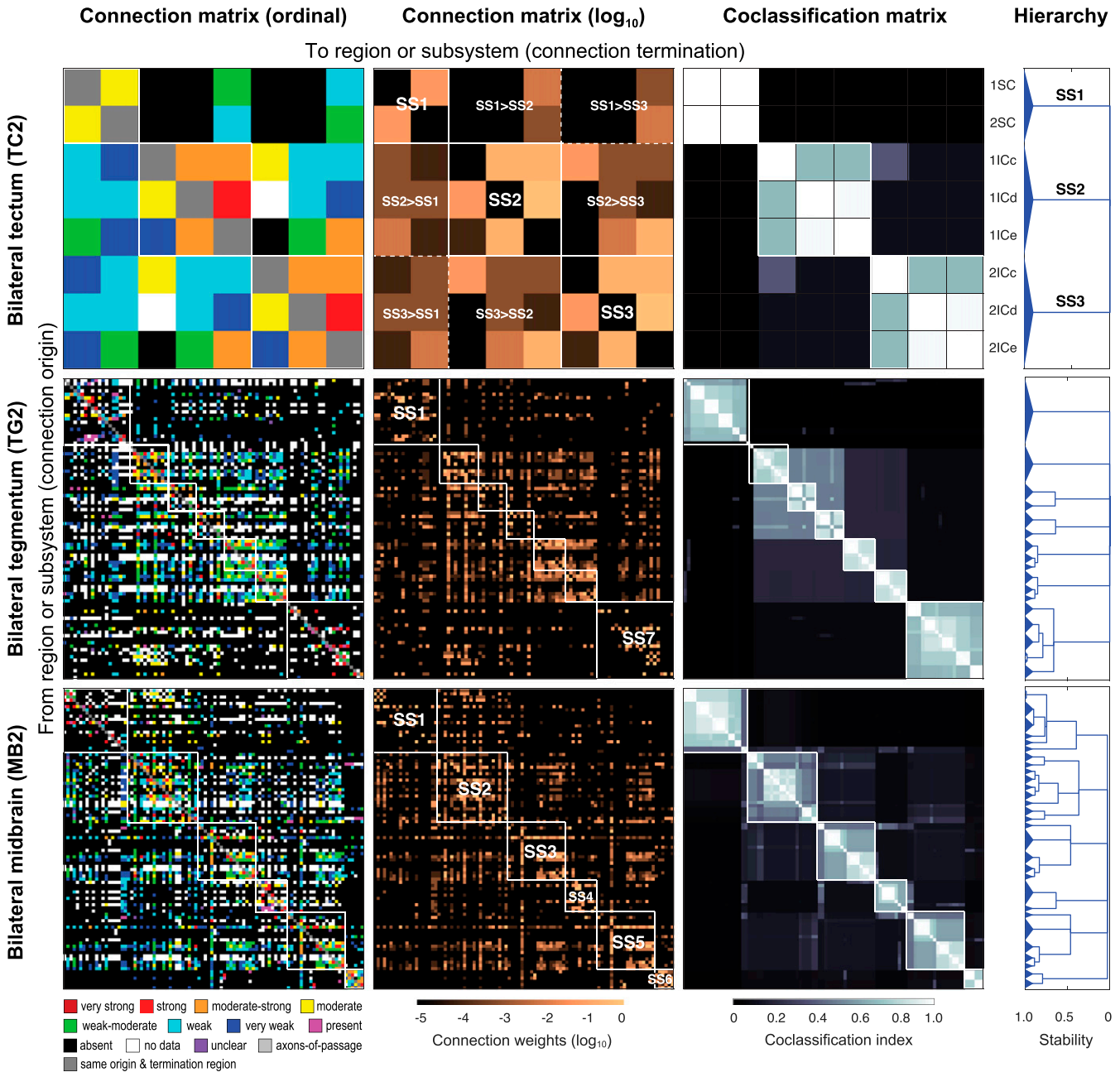

Fig. 2. Bilateral intratectal (TC2), intrategmental (TG2), and intramidbrain (MB2) macroconnectomes. Directed and weighted monosynaptic macroconnection matrices with gray matter region sequence in a subsystem (SS) arrangement derived from multiresolution consensus cluster analysis (MRCC). Collated data are represented by descriptive terms corresponding to ordinal weight values (*Left* column, key at *Bottom*), and then converted to binned log-weighted values (second column) for computation. MRCC of the log-weighted connection data generated coclassification matrices (third column), also represented as a hierarchal dendrogram (right column). Coclassification refers to how consistently a given node (region) pair affiliates with the same network community across all partitions captured by MRCC analysis. The linearly scaled coclassification index covers a range between 0 (no coclassification at any partitioning resolution) and 1 (perfect coclassification across all partitioning resolutions). TC2 has three top-level subsystems (SS1–SS3), TG2 has 7 (SS1–SS7), and MB2 has 6. For TC2, TG2, and MB2 the top-level subsystems are shown across each row; note that each matrix shows the extent of interaction between subsystems, as indicated for the TC2 $\log_{10}$ connection matrix. In an MRCC hierarchy, a branch set's length represents a distance between two points, the point where the set was first created and the point where it splits (or the end of the hierarchy is reached); this length may be interpreted as the branch set's stability (or persistence) across the entire hierarchy such that dominant solutions (branch sets more resistant to splitting) have longer branches and fleeting or unstable solutions have shorter branches. All solutions plotted in the tree survive the statistical testing with a significance level of $\alpha = 0.05$. For region (row and column) identity and interactive matrix stacks for TC2, TG2, and MB2, see Datasets S4–S6, respectively. For region abbreviations, see Dataset S1.

result that probably depends on how informative current understanding of functional significance is for the connections in particular subsystems. For example, a relatively straightforward interpretation of the intraforebrain network's subsystem structure–function organization has been proposed (4), whereas the structure–function significance of the intrathalamus (a forebrain subdivision) network's subsystem organization is unclear (20). Here, the tiny TC2 network organization is easy to describe and interpret. Its

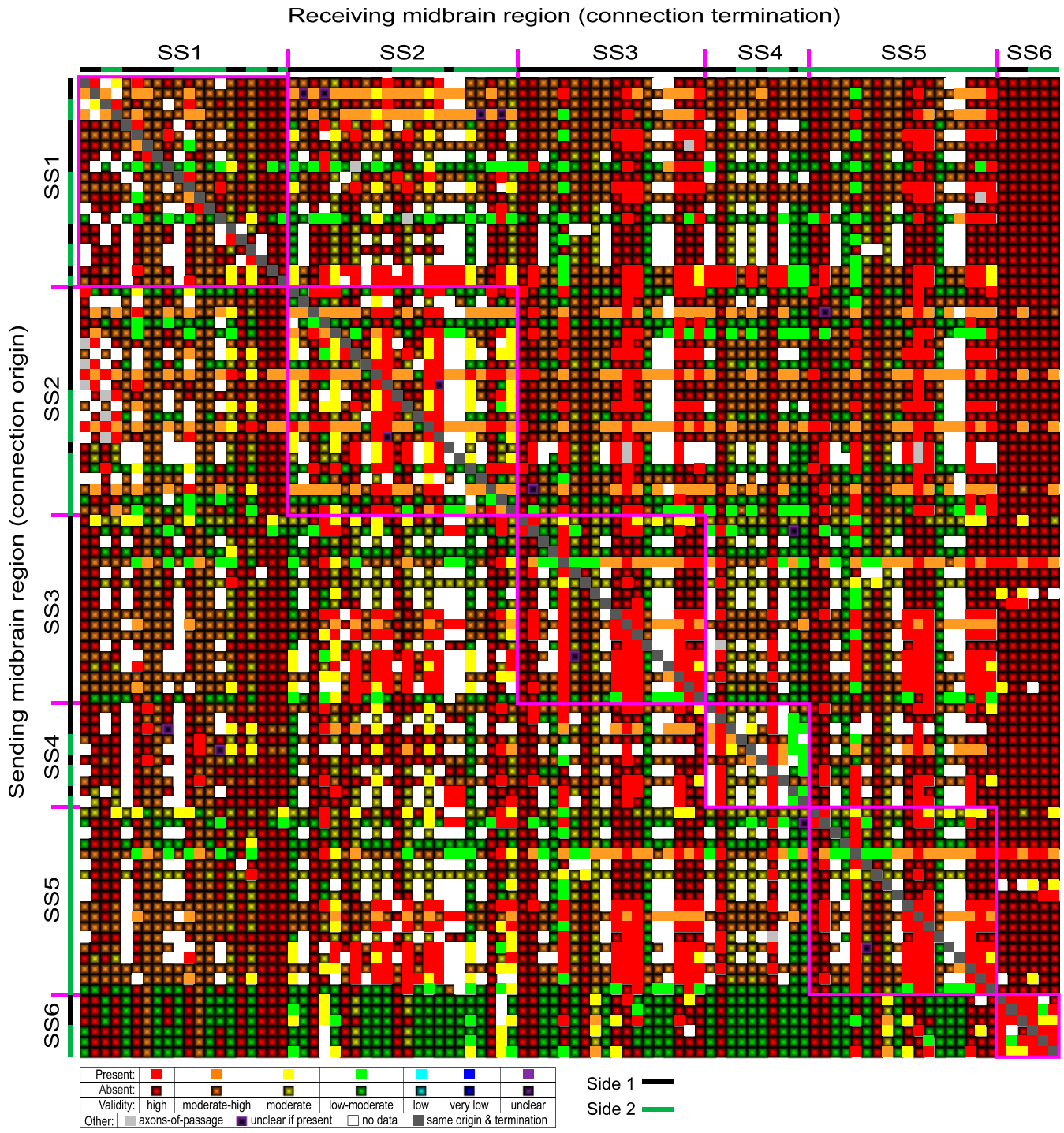

Fig. 3. Comparative matrix of intramidbrain macroconnections and the validity of pathway-tracing methods upon which they are based. The matrix combines a weighted and directed macroconnectome for the bilateral intramidbrain network (MB2) (Fig. 2, *Bottom* row) with a validity measure for the experimental pathway-tracing methods for present or absent connections, based on a seven-point scale (see ref. 4). For absent connections a lower pathway-tracing method validity does not necessarily reduce the validity of the data (see ref. 4). Gray matter region arrangement, side (1 or 2 for left or right, indicated by black and green bars), and top-level subsystems (magenta-delineated subsystems SS1–SS6) are derived from multiresolution consensus cluster analysis (Fig. 2, *Bottom* row, *Right* two columns). A fully expandable version of the matrix, with region order and abbreviations, can be explored in Dataset S6, layers C, D, and I; region abbreviations are defined in Dataset S1.

three-subsystem organization described above in *Subsystem Analysis*, involving the superior and inferior colliculi, has firmly established roles in visual and auditory functionality (3), respectively, that do not need further documentation here.

The possible structure–function interpretation of the TG2 and MB2 subsystem hierarchies are more problematic, based on the most obvious and least controversial functional data (see citations in Dataset S2). In both cases, the region sets in many subsystems contain elements that have not been explicitly associated before, suggesting unexpected functional interactions or correlations but obscuring easy functional assignment based on current evidence. Perhaps not surprisingly, the TG2 subsystem

hierarchy is simpler than the MB2 subsystem hierarchy, although for both hierarchies the functional interpretation is considerably less certain than is the functional interpretation for the intraforebrain (4) and intrahypothalamic (21) subsystem hierarchies. Broadly, the TG appears to be involved primarily in specific motor and more general behavior control, in motivation and reward, and in behavioral state control (Dataset S5). Four of the seven top-level subsystems (SS3–SS6) form two bilaterally symmetrical subsystem pairs. One pair is characterized by the substantia nigra and retrorubral area, and it is clear that the reticular part of substantia nigra is involved in somatomotor control mechanisms, whereas the other pair is dominated by most regions of the periaqueductal gray, and the parts of this pair have been implicated especially in a variety of agonistic and reproductive behaviors.

The other three top-level subsystems of TG2 are bilateral, with virtually the same components on each side. SS1 has no children and is thus quite stable (Fig. 2, *Middle* row, *Right* column). With no children, it also forms the largest bottom-level cluster, containing 19 regions. It is dominated by the red nucleus and regions associated with controlling eye movements, the pupil, and lens accommodation. SS2 also has no children so that its 11 member regions also form a relatively very stable bottom-level subnetwork. The best-known region in SS2 is the ventral tegmental area, suggesting a prominent role in motivation and reward mechanisms. Finally, SS7 divides into six bottom-level subsystems and appears to have heterogeneous functional attributes. They include modulation of behavioral state (midbrain raphe nuclei), locomotion (midbrain reticular nucleus parvicellular part), and extraocular muscle contraction (trochlear nucleus).

Midbrain Structure–Function Model. As expected (see Subsystem Analysis above), combining the TC2 and TG2 subconnectomes to produce the MB2 subconnectome yielded a unique subsystem hierarchy (Fig. 2). Detailed examination of this hierarchy (Dataset S6) revealed the same functional attributes attributed to the TG2 subsystem hierarchy (specific motor and more general behavior control, motivation and reward, and behavioral state control), with the addition of auditory sensory functionality. For the MB2 structure–function subsystem hierarchy model there are six top-level subsystems, one pair of bilaterally symmetrical subsystems (SS3 and SS5), and four subsystems with identical bilateral components (SS1, SS2, SS4, and SS6). The most prominent members of the bilaterally symmetric pair (SS3 and SS5) are the superior colliculus, red nucleus, and most parts of the periaqueductal gray, clearly implicating this subsystem in visual sensory–motor mechanisms and somatic motor control, including complex reproductive and agonistic behavioral responses (see Dataset S2 for citations).

The first bilateral subsystem (SS1) is the most complex, with seven bottom-level subsystems that include the midbrain raphe and interpeduncular nucleus (presumably behavioral state control), the midbrain reticular nucleus parvicellular part (presumably locomotor control), and the trochlear nucleus and Edinger–Westphal nucleus (eye functionality). The second bilateral subsystem (SS2) is dominated by the substantia nigra and ventral tegmental area, which have been associated with motivation and reward. The third bilateral subsystem (SS4) contains the oculomotor nuclei and related regions, and this subsystem is clearly associated with extraocular muscle coordination. And the fourth bilateral subsystem (SS6) consists of the right and left inferior colliculi. It is the simplest, most stable top-level subsystem, with the most straightforward functional attribution: auditory sensory "relay." In addition, SS6 has fewer interactions (input–output connections) with other subsystems than any other top-level subsystem (Dataset S6, layers C–E).

As with the thalamus (20), it seems likely that the structure–function organization of the intra-MB network will be greatly clarified when its extrinsic connections with the rest of the central nervous system are taken into account. That is, the intra-MB network may be less functionally autonomous than, for example, the intraforebrain or intrahypothalamic networks, where the functional significance is more readily apparent (see *Hierarchical Structure–Function Subsystem Models* above).

Subsystem Spatial Relationships. For some brain subdivisions, such as the cerebral cortex (14) and forebrain as a whole (4), the region members of each top-level subsystem clearly segregate spatially, rather than distributing in a checkerboard fashion through the whole subdivision. Visual inspection of our reference atlas (16) shows that, for the present analysis, clear spatial segregation for an entire subconnectome only applies to TC2, as the description of its structure–function subsystem organization suggests (see *Hierarchical Structure–Function Subsystem Models* above), and a flatmap display of its spatial distribution graphically illustrates (Fig. 4*A* and also see Dataset S3, worksheets 4 and 5).

In contrast, the subsystem hierarchies for the much larger TG2 and MB2 subconnectomes display a hybrid pattern, with most or all region members of some top-level subsystems forming an irregularly shaped spatial aggregate and the region members of other top-level subsystems being distributed in a more or less dispersed, unaggregated way. For the TG2 subsystem conformation (Dataset S5), complete spatial aggregation is displayed by the two bilaterally symmetrical pairs of top-level subsystems (SS3 and SS6, associated with motor and complex behavior control), and one bilateral top-level subsystem (SS2, associated with motivation and reward). Parts of the other two top-level subsystems (SS1 and SS7, associated with other motor functions, including locomotor control, and with behavioral state) are spatially discontinuous.

When the entire MB2 network is considered, only two of the six top-level subsystems form spatially aggregated region clusters and both of them are bilateral, with the same region set on each side of the brain (Fig. 4*B*). SS6 (Dataset S6, layers C–E) is the simplest and consists of the right and left inferior colliculus. The other, SS2 (Dataset S6, layers C–E), is considerably more complex but is dominated by the substantia nigra and ventral tegmental area, suggesting that this top-level subsystem plays a role in mechanisms underlying motivation and reward. The region sets of the other four top-level MB2 subsystems are not spatially contiguous, and they display varying degrees of spatial dispersion or nonadjacency.

Global Network Features. To gain further insight into global organizing features of the intra-MB connectome, three basic network attributes were also examined. The first attribute is network centrality, which suggests the relative importance of regions (nodes) in a network, with the most central referred to as hubs. Our identification of hubs was based on aggregated rankings across four regional/nodal centrality measures (degree, strength, betweenness, and closeness) (*SI Appendix*, Fig. S2); after ranking regions on each metric, an aggregate "hub score" was determined for each region by calculating the number of times each region appeared in the top 20% for each centrality measure (13). Using this criterion, eight top-ranked putative hubs (with a hub score of 4) were identified, consisting of four mirror-image region pairs. One pair, the superior colliculi, is in the tectum, whereas the other three pairs form spatially compact right and left units consisting of the ventral tegmental area, retrorubral area, and midbrain reticular nucleus magnocellular part, as can be appreciated on a flatmap (22) (Fig. 5). The superior colliculi play a well-known role in visual sensory–motor mechanisms, whereas the other three putative hubs are elements of MB2's bilateral SS2, and thus play a role in motivation and reward mechanisms, among other functions (see *Hierarchical Structure–Function Subsystem Models* above).

The second network attribute is the so-called "rich club," which refers to a set of individually highly connected nodes that are also mutually highly interconnected (23). The innermost shell of the rich club contains two mirror-image sets of eight members (Fig. 5).

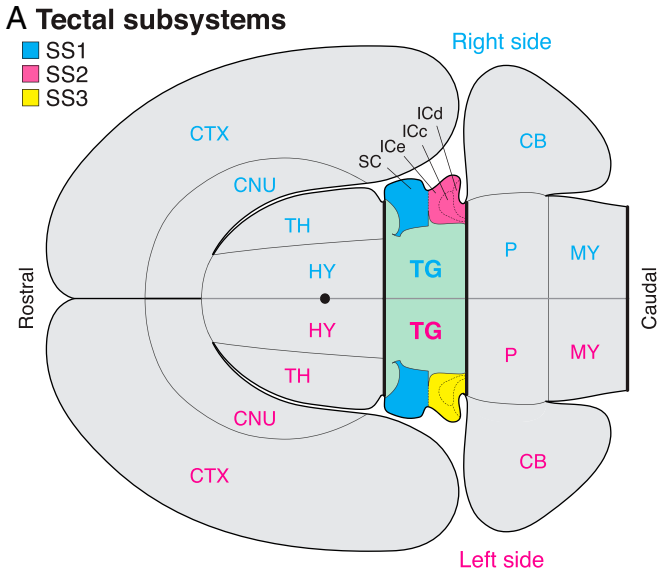

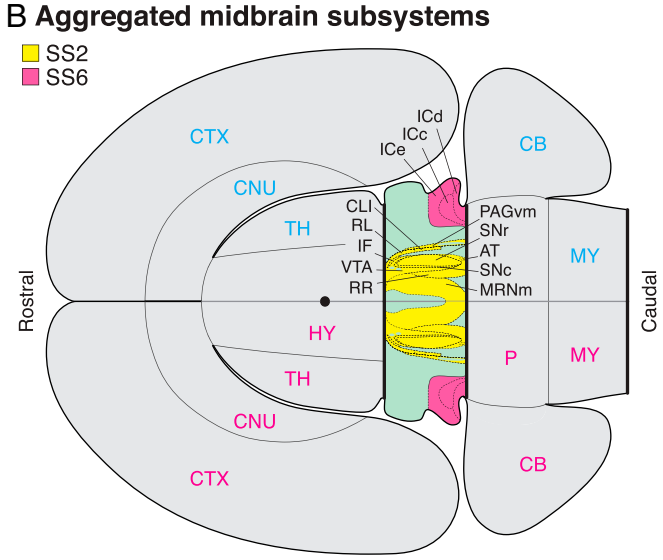

Fig. 4. Spatial distribution of structure–function subsystems displayed on a flatmap of the adult rat brain (Fig. 1*D*). (*A*) The three subsystems associated with the TC2 network. Note that SS1 is bilateral, and includes the right and left superior colliculi (SC), whereas SS2 and SS3 form a bilaterally symmetrical pair, each containing the three regions of the inferior colliculus (IC), external (ICe), central (ICc), and dorsal (ICd). (*B*) The two top-level subsystems associated with the MB2 network that form spatially aggregated (continuous) masses in the three-dimensional brain parenchyma. Note that both of them (SS2 and SS6) are bilateral, containing the same region sets on the two sides of the brain. For clarity, the cuneiform nucleus of SS2 is not illustrated; at one point in the three-dimensional brain the cuneiform nucleus is adjacent to the midbrain reticular nucleus magnocellular part (MRNm) but it was not possible to display this relationship on the two-dimensional flatmap. See Fig. 1*B* and Dataset S1 for abbreviations.

Three of these rich club members are also among the highest-ranking putative hubs just discussed (the superior colliculus, ventral tegmental area, and midbrain reticular nucleus magnocellular part). But interestingly, the other five members are all within the periaqueductal gray, in regions (the precommissural nucleus, and the ventromedial, ventrolateral, lateral, and dorsolateral columns) implicated in the expression of reproductive and agonistic behaviors, nociception, and autonomic responses. Coordinated involvement of the superior colliculi and periaqueductal gray in agonistic behavior is well known (24).

The third network attribute, "small world," applies to networks with highly clustered nodes connected by short paths (25). The MB2 subsystem shows considerably weaker small-world organization than that reported for the bilateral forebrain subsystem and is about the same as that reported for the bilateral hypothalamic (21) and bilateral interbrain (26) subsystems (Fig. 6). As noted above in *Subsystem Spatial Relationships*, the overall subsystem organization of the MB2 network is considerably more fragmented spatially than that of the bilateral forebrain network, consistent with a relatively low mean clustering coefficient for the MB2 network.

Discussion

There are three main findings of the present analysis. First, current data suggest that the intramidbrain macronetwork has a connection density of about 19%; that is, about 19% of all possible connections between its 94 gray matter regions (nodes) are actually formed in the adult, and that this network has four bilaterally symmetrical pairs of hubs (especially highly connected and highly central gray matter regions). Second, cluster analysis has identified within the intramidbrain network a set of 50 subsystems arranged in a structure–function hierarchy with 6 subsystems at the top and 30 subsystems at the bottom. Current analysis combined with annotations from the literature suggest a model wherein these intramidbrain subsystems play distinct functional roles in sensory–motor mechanisms, motivation and reward, regulating complex reproductive and agonistic behaviors, and behavioral state control. And third, the component gray matter regions of some top-level subsystems are spatially contiguous, whereas the components of other subsystems are spatially discontinuous.

It is interesting to compare the organization of MB intrinsic axonal connectivity with that recently described with the same methodology for the forebrain (4). Taken together, five features serve to indicate that the adult forebrain and midbrain have distinct connectional architectures. The first difference is simply the size and extent of regionalization. The MB has the smallest volume of the three major brain divisions in mammals and also has the smallest number of regions, with 94 on both sides of the rat brain, according to the reference atlas used here. In contrast, the bilateral forebrain (FB2) is much larger, primarily because of the cerebral hemispheres, and it has 466 regions according to the

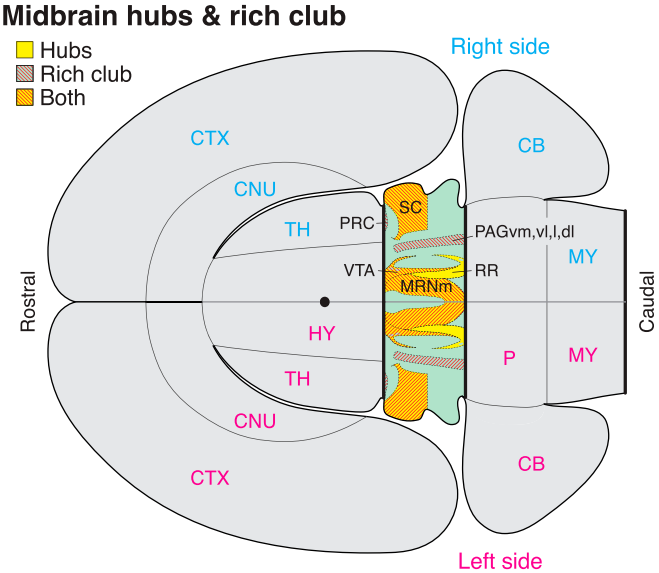

Fig. 5. Spatial distribution of the eight candidate hubs (four mirror-image pairs), and 16 inner circle rich club members (eight mirror-image pairs) for the MB2 network on a flatmap of the rat brain (Figs. 1 and 4). See Fig. 1*B* and Dataset S1 for abbreviations.

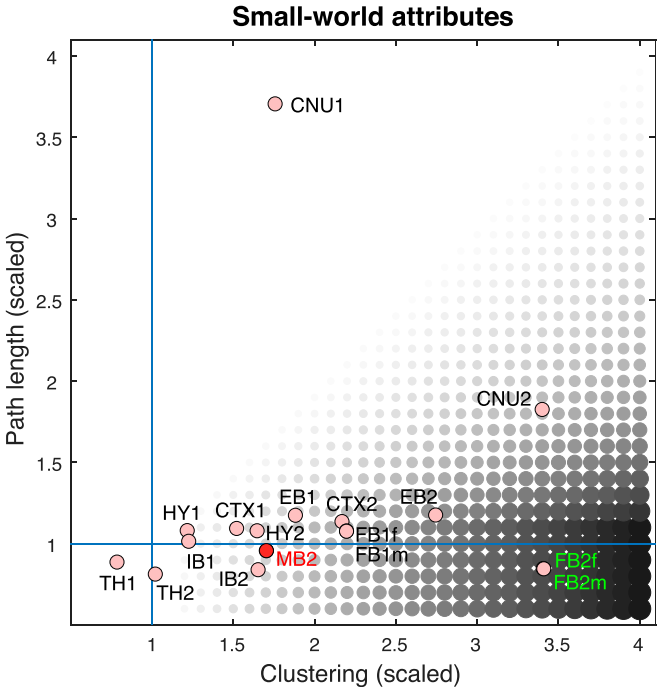

Fig. 6. Comparison of small-world analysis of MB2 with analyses of the forebrain and its major subdivisions. Small-world networks have two main properties: highly clustered (densely interconnected) nodes and relatively short paths between nodes. Clustering is computed as the nodal mean of the weighted and directed clustering coefficients and path length is computed as the global mean of the weighted path lengths between all node pairs. Both metrics are scaled by the corresponding measures' medians from 1,000 degree-preserving randomized networks. The gray circle diameters and their grayness correspond to the ratio between scaled clustering and scaled path length, the small-world index (SWI) (25). For a network to display small-world attributes, its SWI should be >1, with a high (scaling >> 1) clustering index and a short (scaling near 1) path length. For comparison, values are also plotted for previously reported subconnectomes: endbrain (EB1 and EB2) (19) and its component parts, cerebral nuclei (CNU1 and CNU2) (15), and cerebral cortex (CTX1 and CTX2) (14); interbrain (IB1 and IB2) (26) and its component parts, hypothalamus (HY1 and HY2) (21), and thalamus (TH1 and TH2) (20); and FB2 (male, m; female, f) (4), which has the highest SWI of all items plotted.

same atlas. Second, despite a much smaller connection matrix, the MB2 network is differentiated into six top-level subsystems, whereas the FB2 network has only two mirror-image top-level subsystems. Third, specific functional correlates of the MB2 subsystem arrangement are less obvious than those proposed for the FB2 subsystem. Fourth, of the six top-level subsystems in MB2, only two are spatially contiguous, accounting for 28/94 regions. In contrast, there is almost complete spatial aggregation of the 466 regions in the two top-level FB2 subsystems. And fifth, the MB2 network displays relatively weak small-world organization compared to the relatively strong small-world organization characteristic of the FB2 network.

The global structure–function model of intra-MB subsystem organization proposed here is not as easily interpretable as the models proposed for cerebral cortical association (13), intrahypothalamic (21), and intraforebrain (4) subsystem organization. Upper-level FB2 subsystems split functionally and in a spatially compact way into two components, one related to a lateral forebrain system associated primarily with voluntary behavior and cognition, and the other related to a medial forebrain system associated with coordinating instinctive survival behaviors, appropriate physiological responses, and affect. This dual organizational feature is not evident in the isolated MB2 network, which lies caudally adjacent to the FB2 network. However, relative functional ambiguity like that associated with the intra-MB2 subconnectome was also encountered using the same methodology for the thalamus (20). In this case it was suggested that a better understanding of a brain subdivision's structure–function organization may depend critically on taking into account its extrinsic input and output connections with the rest of the central nervous system, and it seems likely that this same principle applies to the MB. We will be in a better position to test this hypothesis systematically when subconnectomes are added to assemble comparable network models of the brain, the central nervous system, and finally the nervous system as a whole.

Major limitations of the methodology used here have been discussed elsewhere (20). Briefly, they include the inevitable development of better pathway-tracing methods, and thus more accurate data; the extension of this macroconnectomics level of analysis to the meso (neuron types) and micro (individual neurons) levels of analysis; the fact that network features do not stabilize until the entire network (the nervous system connected to the rest of the body, the neurome) is analyzed; and the lack of an accompanying dynamic network model. In addition, two other factors are obvious. First, not all possible connections in the MB2 subconnectome have been examined experimentally—we found no data for 11.1% of all possible MB2 connections. Thus, it is likely that when these data are added, some of the lower-level subsystems, at least, of the MB2 subconnectome will be altered. By comparison, no data were found for only 5.2% of all possible FB2 connections (4), whereas that figure was 12.3% for the intrahypothalamic network (21). And second, very rarely has a set of pathway tracer injections covered the entire volume of a region of interest, leaving open the possibility of false negative information for a connection matrix. Conversely, some connection data are based on pathway tracer injections with slight involvement of adjacent regions, leaving open the possibility of false positive connection data.

While there are many limitations to the connectomics approach, one great advantage is that connection matrices aim to provide comprehensive and uniform coverage, and thus encourage tabulating everything that is known, and not known, about structural connectivity of a network of interest—which can then be subjected to formal network analysis. Perhaps the last thorough, critical review focused specifically on midbrain structure–function organization was published almost 60 y ago (27), and it cited about 50 intramidbrain connections, identified with lesion-induced degeneration methods before the introduction of intraaxonal pathway-tracing methods a decade later. This contrasts with the 1,676 intramidbrain connections collated here for the rat from papers published since 1977. It seems unlikely that the organizing principles of circuitry this complex can be deciphered manually, without the aid of formal network analysis tools, and the results of such analysis, particularly the structure–function subsystem hierarchies provided by the MRCC algorithm, offer a powerful, previously unavailable, approach to hypothesis-driven circuit analysis.

To help interpret structure–function subsystem hierarchies for hypothesis-driven circuit analysis we have proposed five core hypotheses (4). First, distinct subsystems (clusters) are distinguished by distinct structural connection sets and thus display unique functional properties. Second, these structure–function subsystems interact within a hierarchically organized global framework. Third, if a subsystem is assigned a provisional function based on a relatively clear functional association of one or more of its regions, then other regions with less clear functional associations are hypothesized to contribute holistically to the assigned subsystem functionality. Fourth, if a parent (higher level) subsystem has two or more children or descendent (immediately lower level) subsystems with distinct functional attributes, then the parent subsystem is hypothesized to possess functional attributes of all the children subsystems. And fifth, if a parent subsystem has two children subsystems, one with a clear functional attribution and one without, then the parent subsystem is hypothesized to possess the known and unknown functions of its children subsystems. Literature supporting the provisional functional

attributions here can be found in the articles cited in Dataset S2, and the structure–function models proposed should be taken simply as versions 1.0, subject to future elaboration.

Materials and Methods

All connection report collation and network analysis methods not outlined in the text, and in *SI Appendix, Materials and Methods*, were thoroughly described previously (4).

Data Availability. All connection report metadata are in a Microsoft Excel spreadsheet (Dataset S2), as are all data from the reports used for connection matrices (Dataset S3). Searchable connection report data are freely available at The Neurome Project (https://sites.google.com/view/the-neurome-project/home) or Dryad (https://doi.org/10.5061/dryad.c866t1g6r). Network analyses were done on the TC2, TG2, and MB2 connection matrices (Dataset S3, worksheet "MB2 topographic bins") with tools collected in the Brain Connectivity Toolbox (https://sites.google.com/site/bctnet/).

1. K. E. von Baer, *Über Entwickelungsgeschichte der Thiere, Beobachtung und Reflexion* (Bornträger, Königsberg, 1837), Part 2.
2. G. Alvarez-Bolado, L. W. Swanson, *Developmental Brain Maps: Structure of the Embryonic Rat Brain* (Elsevier, Amsterdam, 1996).
3. R. Nieuwenhuys, J. Voogd, C. van Huijzen, *The Human Central Nervous System* (Springer, Berlin), ed. 4, 2008).
4. L. W. Swanson, J. D. Hahn, O. Sporns, Structure-function subsystem models of female and male forebrain networks integrating cognition, affect, behavior, and bodily functions. *Proc. Natl. Acad. Sci. U.S.A.* **117**, 31470–31481 (2020).
5. L. W. Swanson, What is the brain? *Trends Neurosci.* **23**, 519–527 (2000).
6. L. W. Swanson, *Neuroanatomical Terminology: A Lexicon of Classical Origins and Historical Foundations* (Oxford University Press, Oxford, 2015).
7. L. W. Swanson, M. Bota, Foundational model of structural connectivity in the nervous system with a schema for wiring diagrams, connectome, and basic plan architecture. *Proc. Natl. Acad. Sci. U.S.A.* **107**, 20610–20617 (2010).
8. O. Sporns, G. Tononi, R. Kötter, The human connectome: A structural description of the human brain. *PLOS Comput. Biol.* **1**, e42 (2005).
9. O. Sporns, *Networks of the Brain* (MIT Press, Cambridge, MA, 2011).
10. D. H. Meadows, *Thinking in Systems: A Primer* (Chelsea Green, White River Junction, VT, 2008).
11. J. W. Lichtman, J. R. Sanes, Ome sweet ome: What can the genome tell us about the connectome? *Curr. Opin. Neurobiol.* **18**, 346–353 (2008).
12. L. W. Swanson, J. W. Lichtman, From Cajal to connectome and beyond. *Annu. Rev. Neurosci.* **39**, 197–216 (2016).
13. M. Bota, O. Sporns, L. W. Swanson, Architecture of the cerebral cortical association connectome underlying cognition. *Proc. Natl. Acad. Sci. U.S.A.* **112**, E2093–E2101 (2015).
14. L. W. Swanson, J. D. Hahn, O. Sporns, Organizing principles for the cerebral cortex network of commissural and association connections. *Proc. Natl. Acad. Sci. U.S.A.* **114**, E9692–E9701 (2017).
15. L. W. Swanson, O. Sporns, J. D. Hahn, Network architecture of the cerebral nuclei (basal ganglia) association and commissural connectome. *Proc. Natl. Acad. Sci. U.S.A.* **113**, E5972–E5981 (2016).
16. L. W. Swanson, Brain maps 4.0–Structure of the rat brain: An open access atlas with global nervous system nomenclature ontology and flatmaps. *J. Comp. Neurol.* **526**, 935–943 (2018).
17. R. A. Brown, L. W. Swanson, Neural systems language: A formal modeling language for the systematic description, unambiguous communication, and automated digital curation of neural connectivity. *J. Comp. Neurol.* **521**, 2889–2906 (2013).
18. L. G. S. Jeub, O. Sporns, S. Fortunato, Multiresolution consensus clustering in networks. *Sci. Rep.* **8**, 3259 (2018).
19. L. W. Swanson, J. D. Hahn, L. G. S. Jeub, S. Fortunato, O. Sporns, Subsystem organization of axonal connections within and between the right and left cerebral cortex and cerebral nuclei (endbrain). *Proc. Natl. Acad. Sci. U.S.A.* **115**, E6910–E6919 (2018).
20. L. W. Swanson, O. Sporns, J. D. Hahn, The network organization of rat intrathalamic macroconnections and a comparison with other forebrain divisions. *Proc. Natl. Acad. Sci. U.S.A.* **116**, 13661–13669 (2019).
21. J. D. Hahn, O. Sporns, A. G. Watts, L. W. Swanson, Macroscale intrinsic network architecture of the hypothalamus. *Proc. Natl. Acad. Sci. U.S.A.* **116**, 8018–8027 (2019).
22. J. D. Hahn *et al.*, An open access mouse brain flatmap and upgraded rat and human brain flatmaps based on current reference atlases. *J. Comp. Neurol.* **529**, 576–594 (2021).
23. V. Colizza, A. Flammini, M. A. Serrano, A. Vespignani, Detecting rich-club ordering in complex networks. *Nat. Phys.* **2**, 110–115 (2006).
24. R. Bandler, A. Depaulis, "Midbrain periaqueductal gray control of defensive behavior in cat and rat" in *The Midbrain Periaqueductal Gray Matter*, A. Depaulis, R. Bandler, Eds. (Springer, Boston, 1991), pp. 175–198.
25. M. D. Humphries, K. Gurney, Network 'small-world-ness': A quantitative method for determining canonical network equivalence. *PLoS One* **3**, e0002051 (2008).
26. L. W. Swanson, O. Sporns, J. D. Hahn, The network architecture of rat intrinsic interbrain (diencephalic) macroconnections. *Proc. Natl. Acad. Sci. U.S.A.* **116**, 26991–27000 (2019).
27. E. C. Crosby, T. Humphrey, E. W. Lauer, *Correlative Anatomy of the Nervous System* (Macmillan, New York, 1962), pp. 221–265.